

## RESEARCH ARTICLE

# Assessing the reliability of MRI-CBCT image registration to visualize temporomandibular joints

<sup>1</sup>M A Q Al-Saleh, <sup>2</sup>J L Jaremko, <sup>1</sup>N Alsufyani, <sup>2</sup>Z Jibri, <sup>1</sup>H Lai and <sup>1</sup>P W Major

<sup>1</sup>School of Dentistry, Faculty of Medicine and Dentistry, University of Alberta, Edmonton, AB, Canada; <sup>2</sup>Department of Radiology and Diagnostic Imaging, Faculty of Medicine and Dentistry, University of Alberta, Edmonton, AB, Canada

**Objectives:** To evaluate image quality of two methods of registering MRI and CBCT images of the temporomandibular joint (TMJ), particularly regarding TMJ articular disc–condyle relationship and osseous abnormality.

**Methods:** MR and CBCT images for 10 patients (20 TMJs) were obtained and co-registered using two methods (non-guided and marker guided) using Mirada XD software (Mirada Medical Ltd, Oxford, UK). Three radiologists independently and blindly evaluated three types of images (MRI, CBCT and registered MRI-CBCT) at two times ( $T_1$  and  $T_2$ ) on two criteria: (1) quality of MRI-CBCT registrations (excellent, fair or poor) and (2) TMJ disc–condylar position and articular osseous abnormalities (osteophytes, erosions and subcortical cyst, surface flattening, sclerosis).

**Results:** 75% of the non-guided registered images showed excellent quality, and 95% of the marker-guided registered images showed poor quality. Significant difference was found between the non-guided and marker-guided registration ( $\chi^2 = 108.5$ ;  $p < 0.01$ ). The interexaminer variability of the disc position in MRI [intraclass correlation coefficient (ICC) = 0.50 at  $T_1$ , 0.56 at  $T_2$ ] was lower than that in MRI-CBCT registered images [ICC = 0.80 (0.52–0.92) at  $T_1$ , 0.84 (0.62–0.93) at  $T_2$ ]. Erosions and subcortical cysts were noticed less frequently in the MRI-CBCT images than in CBCT images.

**Conclusions:** Non-guided registration proved superior to marker-guided registration. Although MRI-CBCT fused images were slightly more limited than CBCT alone to detect osseous abnormalities, use of the fused images improved the consistency among examiners in detecting disc position in relation to the condyle.

*Dentomaxillofacial Radiology* (2015) **44**, 20140244. doi: 10.1259/dmfr.20140244

**Cite this article as:** Al-Saleh MAQ, Jaremko JL, Alsufyani N, Jibri Z, Lai H, Major PW. Assessing the reliability of MRI-CBCT image registration to visualize temporomandibular joints. *Dentomaxillofac Radiol* 2015; **44**: 20140244.

**Keywords:** TMJ; MRI; CBCT; registration

## Introduction

CBCT has become integral to the field of dentistry, specifically in practices of orthodontics, implant dentistry and oral surgery.<sup>1–4</sup> MRI is the current gold standard imaging tool to analyse the position and morphology of the temporomandibular joint (TMJ) articular disc position and

morphology.<sup>5</sup> MRI is also useful to demonstrate condylar/disc translation on mouth opening, joint effusions and synovitis, as well as to a lesser extent osseous erosions and degenerative joint disease.<sup>6</sup> Concurrently, CBCT imaging has become the gold standard imaging tool for evaluation of TMJ bony changes. Pathological changes such as condylar erosion, fractures, ankylosis, dislocation and osteophytes are optimally viewed on CBCT.<sup>1–4</sup>

TMJ internal derangement is defined as the abnormal position of the articular disc in relation to the condylar

Correspondence to: Dr Mohammed A Q Al-Saleh. E-mail: [m.alsaleh@ualberta.ca](mailto:m.alsaleh@ualberta.ca)

This work was supported by “The Fund for Dentistry” from the School of Dentistry, University of Alberta, Edmonton, AB, Canada.

Received 9 July 2014; revised 17 February 2015; accepted 2 March 2015

head and articular eminence of the temporal bone.<sup>7,8</sup> At imaging, the disc is best seen on MRI and the bone is best depicted on CT. Therefore, to optimally assess for internal derangement, it is conceptually desirable to fuse MRI and CT images. Disc position is often inconsistently reported on MRI. A variety of methods have been reported in the literature attempting to define the disc position in relation to different articular osseous anatomy of the TMJ such as condylar outline, condylar head inclination, depth of glenoid fossa and articular eminence slope.<sup>9–11</sup>

The image's diagnostic value relies on two integral parts: the image's information content and the observer's correct interpretation. Approaches such as increased image resolution, observer calibration, standardized categorization and quantitative assessment methods have been introduced to enhance diagnostic value and reduce the decision-making errors when looking at the position of the TMJ articular disc in a MRI.<sup>9–11</sup>

MRI-CBCT registered images are new to dentistry, and this technique may accurately detect the anatomical changes in the maxillofacial region, TMJ and masticatory muscles. Data can be presented at equal resolution in any plane including the panoramic plane.

The relationship between the articular disc of the TMJ and mandibular condyle or glenoid fossa is often difficult to visualize with sole assessment of MRI particularly for the novice clinician. This finding is supported by the relatively low interexaminer reliability for classification of TMJ internal derangement as previously reported in the literature.<sup>12</sup> Merging MRI and CT images result in a hybrid image that combines key features of both images, and allows better clinical interpretation of the TMJ characteristics,<sup>13</sup> and it stands to reason that registration of MRI and CBCT images will also be beneficial.

Image registration is the alignment of two imaging data sets spatially and displays one fused image on a screen that contains both sources of information. The value of MRI and CT image registration has been investigated in the medical literature and has been found to improve diagnosis, monitoring of disease progression and understanding of pathology involved in the brain and abdominal regions.<sup>14–17</sup> In general, two approaches can be taken to achieve image registration. The first is using skin surface fiducial markers to provide three-dimensional points of reference to register and fuse different images. Fiducial markers, with radio-opaque hydrogel that appears in MR and CBCT images, are used in neurosurgery and radiotherapy intraoperative imaging, with a high level of image registration accuracy when the markers are firmly fixed to the patients.<sup>18,19</sup> The second approach using multimodality image registration with normalized mutual information (MI), which depends on correspondence analysis of statistical dependency of two images where one image can help predict the other, has been successfully applied on CT-MRI.<sup>20</sup>

The purpose of this study was, first, to evaluate the radiologists' impression of quality of the two available methods of MRI-CBCT image registration (non-guided vs marker guided) and, second, to evaluate the reliability of determining TMJ articular disc–condyle relationship and articular osseous abnormality using MRI-CBCT-registered images compared with MRI or CT alone.

## Methods and materials

### *Patients*

A total of 10 adult patients (20 TMJs) with history of TMJ disorders were recruited from the Temporomandibular Disorder/Orofacial Pain Clinic at the University of Alberta, Edmonton, AB, Canada, suspected of having a TMJ anatomic abnormality. The study was approved by the Human Research Ethics Board at the University of Alberta (Pro00032935), and informed consent was obtained from all participants. All patients had MR and CBCT images obtained at the same visit with skin surface-attached fiducial markers (15.0 × 3.5 mm) (IZI Medical Products, Baltimore, MD). Self-adhesive skin-surface fiducial markers were placed in five different places in the face (one at nasal ridge, two at zygomatic cheek bones, two at mandibular angles). Fiducial markers clearly appear in both MRI and CBCT and provide discrete three-dimensional points of reference to reconstruct and register images. Patients kept their mouth closed during imaging using centric occlusion bite stent polyvinylsiloxane material.

### *CBCT protocol*

Each CT scan was acquired in 360° of rotation with proper subject upright positioning with Frankfort plane parallel to the floor and was collimated to avoid radio-sensitive structures (thyroid and orbits). Scans were performed using i-CAT® scanner (Imaging Sciences International, Hatfield, PA) at a medium field of view setting, 16-cm wide, 13 cm in height, scan time of 26 s and 0.25-mm voxel size. This included the maxilla and mandible and both of the TMJ condyles.

### *MRI protocol*

MRI of the TMJ was performed in the supine position without sedation or intravenous contrast administration, by 1.5-T scanner (Siemens AG, Munich, Germany) with a multichannel head array coil. Small field of view (13 × 13 cm) dedicated bilateral closed-mouth oblique sagittal sections were obtained perpendicular to the long axis of the condyle. Proton density-weighted images were obtained with slice thickness of 3 mm; inter-slice gap of 0.3 mm; repetition time/echo time of 1800/11 ms; with typically 14 slices per side.

### *Image registration*

MRI and CBCT digital imaging and communications in medicine files of the 20 TMJs were transferred to

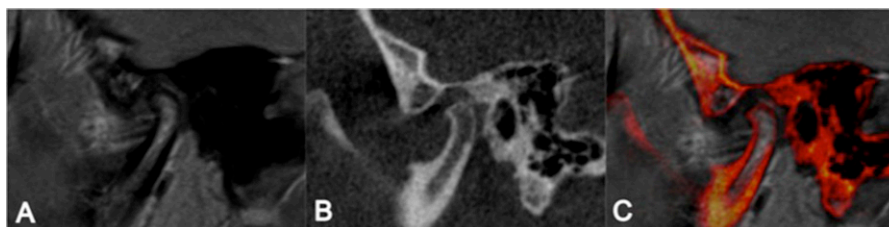


**Figure 1** Sagittal image of the right temporomandibular joint of Subject 9 showing (a) mild anterior disc displacement in the proton density-MR image and (b) flattening of the anterosuperior surface of the condylar head in the CBCT image. (c) CBCT-MR fused image depicts the flattening noted in CBCT image (b) and differentiates condylar-temporal osseous contours from disc tissues noted in the MR image (a).

a desktop computer. Mirada XD software (Mirada Medical Ltd, Oxford, UK) was used to perform multi-modality image registration for MRI and CBCT data sets. Two methods of registration were performed using the software; (1) automatic registration (non-guided) and (2) marker-based automatic registration (marker-guided). In non-guided registration, the two images were brought into a spatial alignment using the MI, and finally fused into a common display (Figure 1).<sup>21</sup>

The marker-guided registration instead depended on identification of the centres of the radio-opaque fiducial markers (torus-shaped with a 1.7-mm central hole diameter) appearing in MRI and CBCT images. Using the two-dimensional axial, coronal and sagittal image sections, the operator would visually locate and mark the centre in one image section and adjust/verify in the remaining two image sections. Both sets of registered images were then saved for assessment.

#### Image assessment

The MRI-CBCT registered images were synthesized by overlying the greyscaled MRI over red colour-coded bony structure of the CBCT image (Figure 1). Three radiologists (ZJ, JJ, NA), with 0, 5 and 8 years of

experience in TMJ image analysis, subjectively evaluated the registered images independently and blindly in two steps. Step 1: examiners subjectively evaluated the quality of image registration (non-guided *vs* marker-guided) and ranked them as excellent, edges of TMJ articular surfaces (condylar head, glenoid fossa and articular eminence) overlap within one pixel; fair, mild variation of the contours and edges of the articular surfaces, mimicking mild motion artefact; poor, large variation of the contours and edges with minimal to no overlap between both images (Figures 2–4). Step 2: examiners evaluated the TMJ disc-condylar relationship and articular osseous abnormalities on MRI, CBCT and MRI-CBCT registered images. To evaluate reliability, two examiners repeated image evaluation twice in a 2-month interval, and the most experienced examiner (NA) repeated the evaluation five times in 2-week intervals. The sagittal position of the articular disc was evaluated following the functional relationship of the disc intermediate zone to the condylar head surface to mild, moderate and full anterior displacement. The categorization guide for the anterior disc position categories in the closed-mouth position are represented in Figure 5. Osseous abnormalities (hyperplasia, hypoplasia), signs of remodelling (surface flattening, sclerosis)

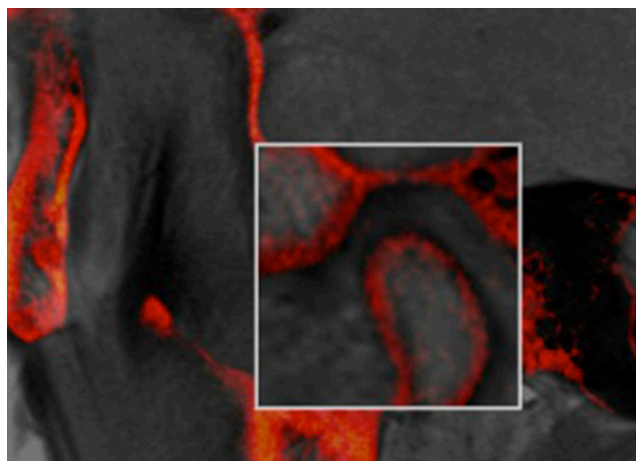


**Figure 2** Sagittal image (MRI-CBCT non-guided registration) of the right temporomandibular joint (TMJ) of Subject 8 showing excellent edges of TMJ articular surfaces (condylar head, glenoid fossa and articular eminence) overlap within 1 pixel.

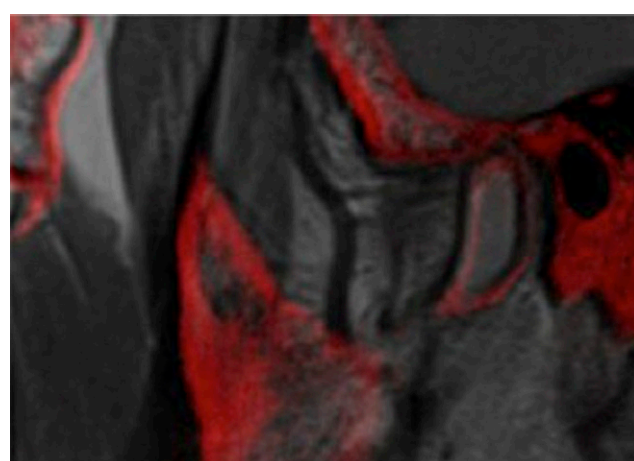


**Figure 3** Sagittal image (MRI-CBCT marker-guided registration) of the right temporomandibular joint of Subject 5 showing imperfect overlap contours and edges of the condyle, mimicking mild motion artefact. Registration quality was ranked as fair.

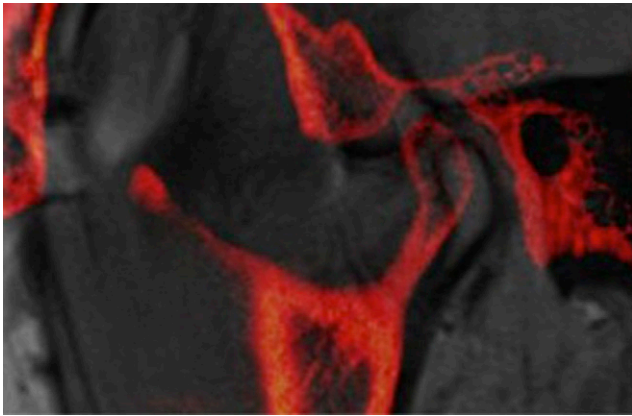


**Figure 4** Sagittal image (MRI-CBCT marker-guided registration) of the right temporomandibular joint of Subject 8 showing poor registration quality with large variation of the contours and edges of the condylar head, glenoid fossa and articular eminence with no overlap between both images.

and degenerative changes (subcortical erosion or cyst, osteophyte, foreign bodies) of the articular surfaces were evaluated and reported.

#### Statistical analysis

The image quality of the registered images was reported in an ordinal scale. A factorial design was devised to

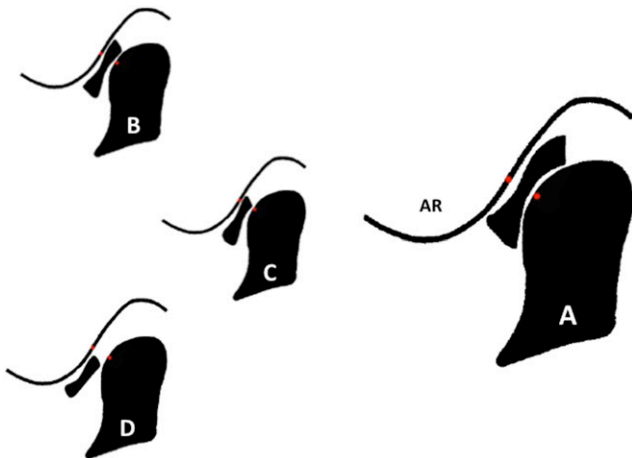


**Figure 5** Illustration of the categories of the anterior disc displacement in closed mouth position. (a) Normal disc position: the intermediate zone of the disc is interposed, in closest point, between the condylar head and posterior slope of the articular eminence (AR), with a “bow-tie” shape of the anterior and posterior bands of the disc. (b) Mild disc displacement: the intermediate zone of the disc is slightly anteriorly displaced. The posterior band of the disc opposed the condylar head. (c) Moderate disc displacement: the intermediate zone of the disc is completely displaced from between the joint osseous structures, or the posterior band of the discs located in the medial or lateral region of the joint. The condylar head is in contact with the junction between the disc posterior band and bilaminar zone. (d) Full displacement: the entire articular disc is anteriorly displaced relative to the posterior slope of the articular eminence and condylar head. The disc bilaminar zone is interposed between the osseous articular structures and occupied the narrowest joint space (represented by the two red dots).

evaluate the quality of images (non-guided vs marker-guided) across different contributing factors (*e.g.* time, examiners and registration type).  $\chi^2$  test results were reported and the level of significance was set at  $p < 0.05$ .

To determine consistency of evaluating the disc position across the three examiners and time, intraclass correlation coefficients (ICCs) were calculated, as the outcome measure was ordinal. To evaluate the consistency of evaluating osseous changes across the three examiners and time, Cohen’s kappa was computed, as the outcome measures were categorical.

## Results

Overall, 75% of the non-guided registered MRI-CBCT images showed excellent image quality whereas only 5% of the marker-guided registered images showed excellent image quality. This difference in quality between the two registration methods was significant,  $\chi^2 = 108.5$  ( $df = 9$ ) and  $p < 0.01$ . Moreover, the assessment of quality of images was not statistically different across examiners or over time ( $p < 0.05$ ). Owing to the high quality of the “non-guided” registered MRI-CBCT images, they were used for the TMJ assessment.

The assessments of disc position of the evaluated images are reported in Tables 1–4. The consistency of disc position evaluation in MRI alone was low between examiners [ICC = 0.50 (0.04–0.78) at  $T_1$  and 0.56 (0.14–0.80) at  $T_2$ ] and high across time ( $T_1$ – $T_2$ ; ICC, 0.80–0.97).

The consistency of disc position evaluation in MRI-CBCT registered images was high among examiners [ICC = 0.80 (0.52–0.92) at  $T_1$ , 0.84 (0.62–0.93) at  $T_2$ ]

**Table 1** Assessment of disc position in MRI at  $T_1$  and intraclass correlation coefficient (ICC) value of the interexaminer consistency

		Examiner 2			
$T_1$		Normal	Mild	Moderate	Severe
Examiner 1	Normal	5	2	1	3
	Mild	2	1	0	0
	Moderate	0	1	0	0
	Severe	0	4	0	1
		Examiner 3			
$T_1$		Normal	Mild	Moderate	Severe
Examiner 1	Normal	1	5	2	3
	Mild	0	1	1	1
	Moderate	0	0	1	0
	Severe	0	0	0	5
		Examiner 3			
$T_1$		Normal	Mild	Moderate	Severe
Examiner 2	Normal	1	3	3	0
	Mild	0	2	1	5
	Moderate	0	1	0	0
	Severe	0	0	0	4

Interexaminer ICC, 50% (4–78%).

Intraexaminer agreement: see  $T_2$ .



**Table 2** Assessment of disc position in MRI at  $T_2$  and intraclass correlation coefficient (ICC) value of the interexaminer consistency

$T_2$		Examiner 2			
		Normal	Mild	Moderate	Severe
Examiner 1	Normal	5	2	1	3
	Mild	2	1	0	0
	Moderate	0	1	0	0
	Severe	0	4	0	1

$T_2$		Examiner 3			
		Normal	Mild	Moderate	Severe
Examiner 1	Normal	1	5	2	3
	Mild	0	1	1	1
	Moderate	0	0	1	0
	Severe	0	0	0	5

$T_2$		Examiner 3			
		Normal	Mild	Moderate	Severe
Examiner 2	Normal	1	3	3	0
	Mild	0	2	1	5
	Moderate	0	1	0	0
	Severe	0	0	0	4

Interexaminer agreement between three examiners: ICC, 56% (14–80%).  
 Intraexaminer agreement—Examiner 1 (two times): ICC, 88% (70–95%); Examiner 2 (two times): ICC, 80% (50–92%); Examiner 3 (five times): ICC, 97% (94–98%).

and high across time (ICC ranged between 0.91 and 0.98).

The consistency in reporting each osseous abnormality across the different examiners and time varied. Inter-examiner agreement on reporting osseous changes was fair to poor ( $k = 0.1–0.5$ ). Substantial to excellent inter-examiner agreement was noticed between the second and third examiners for sclerosis and erosions ( $k = 0.6–0.9$ ).

The average frequency of each osseous abnormality in different image modalities at  $T_1$  and  $T_2$  is summarised in Table 5. Loose intra-articular body was found in only one joint. One examiner reported hyperplasia in two TMJs of one patient and hypoplasia of one TMJ only. The frequency of reporting other abnormalities (osteophytes, erosions and subcortical cyst, surface flattening, sclerosis) was similar between MRI-CBCT images and CBCT images except for slight reduction in the frequency of reporting erosions and subcortical cysts in the MRI-CBCT images.

## Discussion

The process of image registration aims to find a correspondence of each point in a pair of images to spatially align them resulting in a common coordinate frame for both the images. We investigated two methods for performing rigid registration of MRI and CBCT image volumes; both methods were performed in commercially available imaging software (Mirada XD v. 3.6; Mirada Medical Ltd). The first method uses an automated

MI-based algorithm (non-guided registration), and the second uses manually placed markers (marker guided).

The automated non-guided registration is completely automatic and hence eliminates operator bias by using an algorithm to maximize the image match.<sup>14,22</sup> This method does not require operator’s interaction and can be accomplished within seconds.<sup>14</sup> Technically, the process works by automatically adjusting the rigid registration parameters (translation and rotation in three-dimensional) to maximize the MI function, which is a measure of the statistical similarity between the two imaging volumes. During the process, an estimate of the joint histogram is required to calculate the MI function, and for this, linear resampling of the moving image is used. The rigid registration parameters are iteratively refined to increase similarity between both images until optimal/final registration is reached.

The marker-guided registration requires an operator to manually click corresponding locations in the software. Specifically, the user locates the homologous markers in both MRI and CBCT images and specifies those as landmark locations within the software. Once all markers are located, the software can perform an automatic landmark registration, which produces a rigid registration that minimizes the (mean-square) error between all the corresponding landmarks. This method allows some operator interaction to guide registration to maximize the overlap of images.

In both methods, once the images are registered, the quality of image alignment is assessed using a fusion display that shows one image overlaid over the other. Technically, the software uses alpha blending to create the fusion overlay and uses linear image interpolation to resample one image into the space of the other. A

**Table 3** Assessment of disc position in MRI-CBCT at  $T_1$  and intraclass correlation coefficient (ICC) value of the inter-examiner consistency

$T_1$		Examiner 2			
		Normal	Mild	Moderate	Severe
Examiner 1	Normal	1	5	1	2
	Mild	0	3	1	1
	Moderate	0	0	0	0
	Severe	0	0	1	5

$T_1$		Examiner 3			
		Normal	Mild	Moderate	Severe
Examiner 1	Normal	2	5	0	2
	Mild	1	2	0	2
	Moderate	0	0	0	0
	Severe	0	0	0	6

$T_1$		Examiner 3			
		Normal	Mild	Moderate	Severe
Examiner 2	Normal	1	0	0	0
	Mild	2	6	0	0
	Moderate	0	1	0	2
	Severe	0	0	0	8

Interexaminer agreement between three examiners: ICC, 80% (52–92%).  
 Intraexaminer agreement: see  $T_2$ .

**Table 4** Assessment of disc position in MRI-CBCT at  $T_2$  and intraclass correlation coefficient (ICC) value of the inter-examiner consistency

$T_2$		Examiner 2			
		Normal	Mild	Moderate	Severe
Examiner 1	Normal	1	5	1	2
	Mild	0	3	1	1
	Moderate	0	0	0	0
	Severe	0	0	1	5
$T_2$		Examiner 3			
		Normal	Mild	Moderate	Severe
Examiner 1	Normal	2	5	0	2
	Mild	1	2	0	2
	Moderate	0	0	0	0
	Severe	0	0	0	6
$T_2$		Examiner 3			
		Normal	Mild	Moderate	Severe
Examiner 2	Normal	1	0	0	0
	Mild	2	6	0	0
	Moderate	0	1	0	2
	Severe	0	0	0	8

Interexaminer agreement between three examiners: 84% (62–93%).  
Intraexaminer agreement—Examiner 1 (two times): ICC, 91% (80–97%); Examiner 2 (two times): ICC, 96% (89–98%); Examiner 3 (five times): ICC, 98% (97–99%).

transparency tool can be used to adjust the blend between the two volumes, where a user can adjust the intensity-blending ratio as desired.<sup>21</sup>

Colour-coded tissues in MRI and CBCT fused images have been used to evaluate image overlap close to a voxel-size level.<sup>23</sup> Adding fiducial markers to the region of interest with uniform appearance in the MRI and CBCT images is expected to reduce the potential error of the multimodality image registration. However, the rigid registration process does not compensate deformations owing to motion artefact or change in patient's position. In this study, five fiducial markers were fixed to the participants' skin surface, which made them subject to dislocation during imaging. Moreover, the patients' different positions during MRI (supine) vs CBCT (upright) imaging added more error to the registration process. This error in the marker-guided registration explains the marker mismatch between the images, the large variation of the tissue contours and the low quality of the final registration reported by the examiners.

The high signal intensity and complex and unique shapes of the bony structures in the head area clearly provided a reliable foundation for well-defined non-guided image registration. Marker-guided accuracy is reportedly much higher in neurosurgical studies,<sup>24</sup> likely because markers in those studies are attached directly to the bone such as the calvarium by screws, preventing the movements inevitable in use of markers taped to the skin as we did in this study. Results of our study suggest that non-guided registration was clearly superior to marker-guided registration.

MRI has been considered as the prime imaging modality to analyse the soft-tissue changes in the TMJ. However, the accuracy of determining disc position and morphology is challenging and has been the subject of many studies.<sup>11,12,25–27</sup> Proper classification of the disc position improves the diagnostic interpretation of the imaging modality and allows comprehensive use of the provided information. This study used standardized classification of the disc position to improve the consistency of the examiners' disc evaluation.<sup>11</sup>

The fiducial marker displacement during imaging procedure may have affected the MRI-CBCT image alignment and resulted in improper registration with substantial tissue misrepresentation in the final fused image. As a result, the superior quality of the non-guided registered MRI-CBCT images over the marker-guided images rendered the latter inadequate for disc position assessment. Therefore, non-guided registered images were chosen for further analysis and tissue assessment.

The consistency of disc position evaluation, across examiners and time, improved in MRI-CBCT fused images compared with those in MRI alone from 0.50 to 0.80 in  $T_1$  and from 0.56 to 0.84 in  $T_2$ . This can be explained by the fact that disc position (as appeared in MRI) in relation to the condylar head and articular eminence (as appeared in CBCT) were better identified in the MRI-CBCT fused image.

Several measures were introduced over the years to improve the diagnostic accuracy of the disc position in MRI. For instance, imaging hardware and software upgrades, examiner calibration programs and quantification techniques were found to reduce examiners' variability.<sup>10,12</sup> Tasaki and Westesson<sup>28</sup> reported almost perfect agreement ( $k = 0.87$ ) between two examiners in detecting the disc position of 149 TMJs. Orsini *et al*<sup>10</sup>

**Table 5** Frequency average (%) of osseous pathology of 20 temporomandibular joints as reported by examiners in CBCT and MRI-CBCT images

Osseous pathology	Examiner 1		Examiner 2		Examiner 3	
	CBCT	MRI-CBCT	CBCT	MRI-CBCT	CBCT	MRI-CBCT
Hyperplasia	0	0	5	5	0	0
Hypoplasia	0	0	0	5	0	0
Osteophyte	65	65	100	100	90	65
Erosions or subcortical cyst	45	25	75	50	70	50
Surface flattening	25	30	80	75	75	75
Sclerosis	20	10	90	45	65	40
Foreign bodies	5	5	5	5	5	5

reported improvement of agreement among three examiners, to detect disc position in 160 TMJs, after calibration program from moderate ( $k = 0.50$ ) to substantial ( $k = 0.68$ ) agreement. Nebbe *et al*<sup>11</sup> reported moderate to substantial agreement ( $k = 0.49$ – $0.61$ ) for 70 TMJs, when standardized criteria for categorization were used in image analysis. Almost perfect agreement ( $k = 0.91$ ) among the four examiners was demonstrated at the disc displacement without reduction category. Compared with these studies, the relatively lower reliability as seen in this study may be attributed to the small number of cases and the variable experience levels of the radiologists involved.

CBCT has been reported to have excellent ability to evaluate osseous pathology of the TMJ.<sup>29–32</sup> CBCT showed high reliability to detect cortical erosions of the TMJ articular surfaces with 95% accuracy.<sup>30</sup> Alkhader *et al*<sup>33</sup> reported osseous pathology of 106 MRIs of the TMJs evaluated by 2 examiners and determined the sensitivity and specificity of MRI compared with those of CBCT. The mean sensitivity of MRI ranged between 30% and 82%, and the mean specificity ranged between 84% and 98%. The interexaminer agreement was fair ( $k = 0.40$ – $0.59$ ) for all types of osseous pathology, and was poor ( $k < 0.4$ ) for bone sclerosis. Different studies reported fluctuating MRI sensitivity (50–87%) and specificity (71–100%) values to detect osseous pathology.<sup>28,33,34</sup> In this, the findings of this study were not in support of the findings in the literature; examiners showed poor to fair interexaminer agreement in all types of osseous pathology. This range of reported values is attributed to the different imaging protocols, reference test and evaluation methods.

The frequency reporting osseous changes in MRI-CBCT fused images was similar to CBCT images alone for most of the osseous findings of osteophytes, erosions and subcortical cysts, surface flattening, sclerosis (Table 5).

In this study, MRI-CBCT fused images are appropriate to detect changes in osseous morphology; however, CBCT alone may exceed fused MRI-CBCT in detecting minor abnormalities such as erosion. This is attributable to the overlying MR images masking small osseous changes in the MRI-CBCT fused images. Dynamic

windowing and alteration of the relative transparency of the MRI and CBCT components of the fused images by the observer can minimize this effect.

The MRI-CBCT-registered images provide a complementary imaging tool that utilizes the best soft-tissue morphology from MRI and well-defined osseous tissue outline from CBCT.

This study had limitations, chiefly the small sample size and the variability of radiologists' interpretation experience. The wide range of experience of the radiologists assessing the TMJ's was in one sense a limitation, but in another sense, a strength of the study because it demonstrates that MRI-CBCT fusion may improve performance for less experienced radiologists and perhaps compensate somewhat for lack of experience. This hypothesis could be tested more fully in later studies. This study was planned as a pilot project to determine whether the use of such tool enhances the diagnostic value of the TMJ soft-tissue abnormalities in one combined image set. The MRI-CBCT fused image can provide diagnostically useful images for research purposes and may be especially helpful for novice practitioners to detect the disc position in relation to the bony condyle and articular eminence.

## Conclusions

Non-guided registration proved superior to marker-guided registration. The diagnostic value of the MRI-CBCT images to detect osseous abnormality is comparable to CBCT alone except for small osseous changes such as erosions. The MRI-CBCT fused images improved the consistency among examiners of varying experience levels in classifying disc position in relation to the condyle.

## Acknowledgments

The authors would like to thank Mr Timor Kadir, Chief Scientific and Technology Officer at Miranda Medical<sup>®</sup> for his help and guidance.

## References

1. Honda K, Natsumi Y, Sakurai K, Ishikura R, Urade M. Mucinous adenocarcinoma of the temporal region initially diagnosed as temporomandibular disorders: a case report. *J Oral Pathol Med* 2006; **35**: 582–5.
2. Hilgers ML, Scarfe WC, Scheetz JP, Farman AG. Accuracy of linear temporomandibular joint measurements with cone beam computed tomography and digital cephalometric radiography. *Am J Orthod Dentofacial Orthop* 2005; **128**: 803–11.
3. Hintze H, Wiese M, Wenzel A. Cone beam CT and conventional tomography for the detection of morphological temporomandibular joint changes. *Dentomaxillofac Radiol* 2007; **36**: 192–7.
4. Honey OB, Scarfe WC, Hilgers MJ, Klueber K, Silveira AM, Haskell BS, *et al*. Accuracy of cone-beam computed tomography imaging of the temporomandibular joint: comparisons with panoramic radiology and linear tomography. *Am J Orthod Dentofacial Orthop* 2007; **132**: 429–38.
5. Tallents RH, Katzberg RW, Murphy W, Proskin H. Magnetic resonance imaging findings in asymptomatic volunteers and symptomatic patients with temporomandibular disorders. *J Prosthet Dent* 1996; **75**: 529–33.
6. Whyte AM, McNamara D, Rosenberg I, Whyte AW. Magnetic resonance imaging in the evaluation of temporomandibular joint disc displacement—a review of 144 cases. *Int J Oral Maxillofac Surg* 2006; **35**: 696–703.
7. Sanchez-Woodworth RE, Tallents RH, Katzberg RW, Guay JA. Bilateral internal derangements of temporomandibular joint: evaluation by magnetic resonance imaging. *Oral Surg Oral Med Oral Pathol* 1988; **65**: 281–5.
8. Murakami S, Takahashi A, Nishiyama H, Fujishita M, Fuchihata H. Magnetic resonance evaluation of the temporomandibular joint disc position and configuration. *Dentomaxillofac Radiol* 1993; **22**: 205–7.

9. Silverstein R, Dunn S, Binder R, Maganzini A. MRI assessment of the normal temporomandibular joint with the use of projective geometry. *Oral Surg Oral Med Oral Pathol* 1994; **77**: 523–30.
10. Orsini MG, Kuboki T, Terada S, Matsuka Y, Yamashita A, Clark GT. Diagnostic value of 4 criteria to interpret temporomandibular joint normal disk position on magnetic resonance images. *Oral Surg Oral Med Oral Pathol Oral Radiol Endod* 1998; **86**: 489–97.
11. Nebbe B, Brooks SL, Hatcher D, Hollender LG, Prasad NG, Major PW. Magnetic resonance imaging of the temporomandibular joint: interobserver agreement in subjective classification of disk status. *Oral Surg Oral Med Oral Pathol Oral Radiol Endod* 2000; **90**: 102–7.
12. Nebbe B, Brooks SL, Hatcher D, Hollender LG, Prasad NG, Major PW. Interobserver reliability in quantitative MRI assessment of temporomandibular joint disk status. *Oral Surg Oral Med Oral Pathol Oral Radiol Endod* 1998; **86**: 746–50.
13. Dai J, Dong Y, Shen SG. Merging the computed tomography and magnetic resonance imaging images for the visualization of temporomandibular joint disk. *J Craniofac Surg* 2012; **23**: e647–8. doi: [10.1097/SCS.0b013e3182710517](https://doi.org/10.1097/SCS.0b013e3182710517)
14. Pappas IP, Styner M, Malik P, Remonda L, Caversaccio M. Automatic method to assess local CT-MR imaging registration accuracy on images of the head. *AJNR Am J Neuroradiol* 2005; **26**: 137–44.
15. McGahan JP. Challenges in abdominal/pelvic biopsy techniques. *Abdom Imaging* 2013; **38**: 1043–56. doi: [10.1007/s00261-013-0006-8](https://doi.org/10.1007/s00261-013-0006-8)
16. Makino Y, Imai Y, Igura T, Ohama H, Kogita S, Sawai Y, et al. Usefulness of the multimodality fusion imaging for the diagnosis and treatment of hepatocellular carcinoma. *Dig Dis* 2012; **30**: 580–7. doi: [10.1159/000343070](https://doi.org/10.1159/000343070)
17. von Schulthess GK, Kuhn FP, Kaufmann P, Veit-Haibach P. Clinical positron emission tomography/magnetic resonance imaging applications. *Semin Nucl Med* 2013; **43**: 3–10. doi: [10.1053/j.semnuclmed.2012.08.005](https://doi.org/10.1053/j.semnuclmed.2012.08.005)
18. Hamming NM, Daly MJ, Irish JC, Siewerdsen JH. Effect of fiducial configuration on target registration error in intraoperative cone-beam CT guidance of head and neck surgery. *Conf Proc IEEE Eng Med Biol Soc* 2008; **2008**: 3643–8. doi: [10.1109/IEMBS.2008.4649997](https://doi.org/10.1109/IEMBS.2008.4649997)
19. Burkey BB, Speyer MT, Maciunas RJ, Fitzpatrick JM, Galloway RL Jr, Allen GS. Sublabial, transseptal, transphenoidal approach to the pituitary region guided by the ACUSTAR I system. *Otolaryngol Head Neck Surg* 1998; **118**: 191–4.
20. Pawiro SA, Markelj P, Pernus F, Gendrin C, Figl M, Weber C, et al. Validation for 2D/3D registration. I: a new gold standard data set. *Med Phys* 2011; **38**: 1481–90.
21. Egnal G, Daniilidis K. *Image registration using mutual information*. Thesis. University of Pennsylvania; 2000.
22. Studholme C, Hill DL, Hawkes DJ. Automated 3-D registration of MR and CT images of the head. *Med Image Anal* 1996; **1**: 163–75.
23. Pappas IP, Puja M, Styner M, Liu J, Caversaccio M. New method to assess the registration of CT-MR images of the head. *Injury* 2004; **35**(Suppl. 1): S-A105–12.
24. Shamir RR, Joskowicz L, Shoshan Y. Fiducial optimization for minimal target registration error in image-guided neurosurgery. *IEEE Trans Med Imaging* 2012; **31**: 725–37. doi: [10.1109/TMI.2011.2175939](https://doi.org/10.1109/TMI.2011.2175939)
25. Provenzano Mde M, Chilvarquer I, Fenyó-Pereira M. How should the articular disk position be analyzed? *J Oral Maxillofac Surg* 2012; **70**: 1534–9. doi: [10.1016/j.joms.2011.08.004](https://doi.org/10.1016/j.joms.2011.08.004)
26. Pullinger AG, Seligman DA. Multifactorial analysis of differences in temporomandibular joint hard tissue anatomic relationships between disk displacement with and without reduction in women. *J Prosthet Dent* 2001; **86**: 407–19.
27. Nebbe B, Major PW, Prasad NG, Hatcher D. Quantitative assessment of temporomandibular joint disk status. *Oral Surg Oral Med Oral Pathol Oral Radiol Endod* 1998; **85**: 598–607.
28. Tasaki MM, Westesson PL. Temporomandibular joint: diagnostic accuracy with sagittal and coronal MR imaging. *Radiology* 1993; **186**: 723–9.
29. Meng JH, Zhang WL, Liu DG, Zhao YP, Ma XC. Diagnostic evaluation of the temporomandibular joint osteoarthritis using cone beam computed tomography compared with conventional radiographic technology. [In Chinese.] *Beijing Da Xue Xue Bao* 2007; **39**: 26–9.
30. Honda K, Larheim TA, Maruhashi K, Matsumoto K, Iwai K. Osseous abnormalities of the mandibular condyle: diagnostic reliability of cone beam computed tomography compared with helical computed tomography based on an autopsy material. *Dentomaxillofac Radiol* 2006; **35**: 152–7.
31. Tsiklakis K, Syriopoulos K, Stamatakis HC. Radiographic examination of the temporomandibular joint using cone beam computed tomography. *Dentomaxillofac Radiol* 2004; **33**: 196–201.
32. Alexiou K, Stamatakis H, Tsiklakis K. Evaluation of the severity of temporomandibular joint osteoarthritic changes related to age using cone beam computed tomography. *Dentomaxillofac Radiol* 2009; **38**: 141–7. doi: [10.1259/dmfr/59263880](https://doi.org/10.1259/dmfr/59263880)
33. Alkhader M, Ohbayashi N, Tetsumura A, Nakamura S, Okochi K, Momin MA, et al. Diagnostic performance of magnetic resonance imaging for detecting osseous abnormalities of the temporomandibular joint and its correlation with cone beam computed tomography. *Dentomaxillofac Radiol* 2010; **39**: 270–6. doi: [10.1259/dmfr/25151578](https://doi.org/10.1259/dmfr/25151578)
34. Westesson PL, Katzberg RW, Tallents RH, Sanchez-Woodworth RE, Svensson SA. CT and MR of the temporomandibular joint: comparison with autopsy specimens. *AJR Am J Roentgenol* 1987; **148**: 1165–71.